Biochimica et Biophysica Acta 1857 (2016) 1344–1351

Contents lists available at ScienceDirect

Biochimica et Biophysica Acta

journal homepage: www.elsevier.com/locate/bbabio

Clock-genes and mitochondrial respiratory activity: Evidence of a reciprocal interplay☆

Rosella Scrima [a,1], Olga Cela [a,1], Giuseppe Merla [b], Bartolomeo Augello [b], Rosa Rubino [c,d], Giovanni Quarato [a,2], Sabino Fugetto [a], Marta Menga [a], Luise Fuhr [c,d], Angela Relógio [c,d], Claudia Piccoli [a], Gianluigi Mazzoccoli [e,*], Nazzareno Capitanio [a,**]

[a] Department of Clinical and Experimental Medicine, University of Foggia, Foggia, Italy
[b] Medical Genetics Unit, IRCCS "Casa Sollievo della Sofferenza", San Giovanni Rotondo (FG), Italy
[c] Molekulares Krebsforschungszentrum (MKFZ), Charité-Universitätsmedizin Berlin, Germany
[d] Institute for Theoretical Biology (ITB), Charité-Universitätsmedizin Berlin and Humboldt-Universität zu Berlin, Berlin, Germany
[e] Department of Medical Sciences, Division of Internal Medicine and Chronobiology Unit, IRCCS "Casa Sollievo della Sofferenza", San Giovanni Rotondo (FG), Italy

ARTICLE INFO

Article history:
Received 15 December 2015
Received in revised form 25 March 2016
Accepted 29 March 2016
Available online 7 April 2016

Keywords:
Mitochondria
Clock-genes
Oxidative phosphorylation

ABSTRACT

In the past few years mounting evidences have highlighted the tight correlation between circadian rhythms and metabolism. Although at the organismal level the central timekeeper is constituted by the hypothalamic suprachiasmatic nuclei practically all the peripheral tissues are equipped with autonomous oscillators made up by common molecular clockworks represented by circuits of gene expression that are organized in interconnected positive and negative feed-back loops. In this study we exploited a well-established *in vitro* synchronization model to investigate specifically the linkage between clock gene expression and the mitochondrial oxidative phosphorylation (OxPhos). Here we show that synchronized cells exhibit an autonomous ultradian mitochondrial respiratory activity which is abrogated by silencing the master clock gene *ARNTL/BMAL1*. Surprisingly, pharmacological inhibition of the mitochondrial OxPhos system resulted in dramatic deregulation of the rhythmic clock-gene expression and a similar result was attained with mtDNA depleted cells (Rho0). Our findings provide a novel level of complexity in the interlocked feedback loop controlling the interplay between cellular bioenergetics and the molecular clockwork. This article is part of a Special Issue entitled 'EBEC 2016: 19th European Bioenergetics Conference, Riva del Garda, Italy, July 2-6, 2016', edited by Prof. Paolo Bernardi.

1. Introduction

In mammals many physiological processes display rhythmicity endogenously generated by a circadian clock thought to represent an adaptive response which allows organisms to anticipate environmental oscillating changes (light/darkness, feeding/fasting, daily temperature oscillations, *etc.*) or internal endocrine secretion [1]. The main pacemaker controlling the diurnal rhythms is represented by the suprachiasmic nuclei (SCN), which are located in the hypothalamus and receive photic inputs from the retina through the retinohypothalamic tract. The molecular basis of the pacemaker activity of the SCN relays on a relatively low number of clock genes, which act by transcriptional-translational auto-regulatory feedback loops further modulable by epigenetic modifications, miRNA, post-transcriptional and post-translational modifications [2].

The positive limb of the loop is operated by the transcriptional activators CLOCK and *BMAL1* and their target genes Period (*PER1,2,3*) and Cryptochrome (*CRY1,2*), which encode circadian proteins accumulating and forming a repressor complex that interacts with CLOCK-*BMAL1* heterodimers to inhibit their transcriptional activity. The orphan nuclear

Abbreviations: CLOCK, circadian locomotor output cycles kaput; BMAL, brain and muscle aryl hydrocarbon receptor nuclear translocator (ARNT)-like; SNC, suprachiasmic nuclei; PER, period; CRY, cryptochrome; ROR-alpha, RAR-related orphan receptor alpha; NAM, nicotinamide; NAD, nicotinamide adenine dinucleotide; NAMPT, nicotinamide phosphoribosyltransferase; PGC-1α, proliferator-activated receptor gamma coactivator 1-alpha; SIRT, sirtuin (silent mating type information regulation 2 homolog); OxPhos, oxidative phosphorylation; DMEM, Dulbecco's Modified Eagle's Medium; PBS, phosphate-buffered saline; OCR_{RR}, resting oxygen consumption rate; $OCR_{O/L}$, oxygen consumption rate in the presence of oligomycin; OCR_U, uncoupled oxygen consumption rate; FCCP, carbonilcyanide p-triflouromethoxyphenylhydrazone; $\Delta\Psi_m$, mitochondrial membrane electrical potential; Rho0, cells depleted of mitochondrial DNA.

☆ This article is part of a Special Issue entitled 'EBEC 2016: 19th European Bioenergetics Conference, Riva del Garda, Italy, July 2–6, 2016', edited by Prof. Paolo Bernardi.

* Correspondence to: G. Mazzoccoli, Department of Medical Sciences, Division of Internal Medicine and Chronobiology Unit, IRCCS Scientific Institute and Regional General Hospital "Casa Sollievo della Sofferenza", San Giovanni Rotondo (FG), 71013, Italy.
** Correspondence to: N. Capitanio, Department of Clinical and Experimental Medicine, University of Foggia, Foggia, Biomedical Pole "E. Altomare", via Napoli, 71122, Italy.
E-mail addresses: g.mazzoccoli@operapadrepio.it (G. Mazzoccoli), nazzareno.capitanio@unifg.it (N. Capitanio).

[1] Equal contribution.

[2] Present address: Department of Immunology, St Jude Children's Research Hospital, Memphis, TN 38105, USA.

http://dx.doi.org/10.1016/j.bbabio.2016.03.035
0005-2728/

hormone receptors REV-ERBα and RORα operate a feedback loop controlling negatively and positively *BMAL1* transcription, respectively [3].

Accumulating evidences support the notion that the cells of virtually all the peripheral tissues are endowed with autonomous self-sustained molecular oscillators constituted by almost the same clock gene machinery operating in the SCN. The function of the SCN, therefore, is to entrain the phases of the peripheral oscillators [4]. Noticeably, recent evidences show that about half of all protein coding genes in mammals display circadian transcription rhythms largely in an organ-specific manner [5].

The amplitude of oscillation of many clock genes is influenced by SIRT1, a type III histone/protein deacetylase [6], whose activity depends on the oscillating levels of nicotinamide (NAM) adenine dinucleotide (NAD), synthesized in the salvage pathway by the committing nicotinamide phosphoribosyltransferase (NAMPT), whose expression is circadian rhythmic [7,8].

Importantly, peroxisome proliferator-activated receptor gamma coactivator 1-alpha (PGC-1α), a master transcriptional coactivator positively controlling mitochondrial biogenesis and redox homeostasis [9] proved to be a target of SIRT1 thereby providing support for a reciprocal interaction between metabolism and circadian clocks [10,11]. Consistently, recent studies have addressed the role that mitochondrial bioenergetics and dynamics play in cell metabolism in relation to circadian rhythmicity [8,12–14], highlighting the interplay between mitochondrial oxidative phosphorylation (OxPhos) and the functioning of the biological clock and fostering further in-depth analysis.

Aim of the present study was to investigate the mutual impact of circadian clock gene oscillation and the mitochondrial respiratory activity taking advantage of a well-established *in vitro* model of synchronized cultured human cells.

2. Materials and methods

2.1. Cell cultures, "in vitro" synchronization protocol and Rho0 generation

Human hepatoma-derived cell line (HepG2) was obtained from the European Collection of Cell Cultures (ECACC Salisbury, UK); neonatal normal human dermal fibroblasts (NHDF-neo) were from Camb-rex# CC-2509. Cell cultures were maintained at 37 °C in the presence of 5% CO_2 in DMEM (low-glucose Gibco) supplemented with 10 mM Hepes, 10% inactivated fetal bovine serum (FBS), 2 mM glutamine, 100 U/ml of penicillin and 100 μg/ml of streptomycin. For live-cell bioluminescence recording, HepG2 cells were maintained in phenol red-free DMEM supplemented with 250 μM D-Luciferin (PJK). The serum shock induced synchronization was performed in HepG2 and NHDF-neo as in [15]. Briefly: approximately 3×10 [6] cells/dish were plated the day before the experiments. At the day of the experiments, culture medium was exchanged with serum-rich DMEM, containing 50% FBS, for 2 h and then the medium was replaced with serum-free DMEM. The cells were harvested and assayed at the different time points indicated in the text/figures. Cell cultures were typically utilized at a passage number below 18–20 and at a confluence of 80–85%. Rho0 cells were generated from NHDF-neo by cellular exposure to ethidium bromide at low concentration (100 ng/ml) for 40 days and kept in culture in DMEM supplemented with 10% fetal bovine serum, 1 mM pyruvate and 50 mg/ml uridine [16]. Quantification of the mtDNA was carried by PCR amplification of the mtDNA gene ND6.

2.2. Quantitative RT-PCR

Total RNA from HepG2 at different time points was extracted using the RNeasy® Mini Kit (Qiagen S.p.a. Milan, Italy) and subsequently digested by DNase I. cDNA was synthesized from 100 ng total RNA with Quantifast RT-PCR kit (Qiagen). For real-time PCR, we used the following SYBR Green QuantiTect Primers purchased from Qiagen: *ARNTL/BMAL1* (QT00068250); *NR1D1* (RevErbα) (QT00000413). Reactions were set up in 96-well plates using a 7700 Real-Time PCR System (Applied Biosystems, Foster City, CA, USA). Expression levels of the target gene were normalized using the housekeeping control gene TATA binding protein (TBP, QT00000721). mRNA amount of each target gene relative to TBP was calculated through the comparative Ct method (i.e. the $2^{(-\Delta\Delta Ct)}$ method).

2.3. BMAL1-specific siRNA transfection in HepG2 cells

BMAL1-specific siRNA was purchased from Sigma-Aldrich (Mission Pre-designed siRNA2D). HepG2 cells were seeded on 60-mm dishes and at 30–50% confluence were transiently transfected with the *BMAL1*-specific siRNA diluted in Opti-MEM using Lipofectamine® 2000 Transfection Reagent (Invitrogen) according to the manufacturer's protocol. After 6 h of incubation at 37 °C, the transfection medium was replaced with complete medium containing 10% FBS and The experiments were conducted 12 and 24 h later.

2.4. Respirometric measurements

Cultured cells were gently detached from the dish by tripsinisation, washed in PBS, harvested by centrifugation at 500 ×*g* for 5 min and immediately assessed for O_2 consumption with a high resolution oxymeter (Oxygraph-2 k, Oroboros Instruments). About $8–10 \times 10$ [6] viable cells/ml were assayed in DMEM at 37 °C; after attainment of a stationary endogenous substrate-sustained resting oxygen consumption rate (OCR_{RR}), 2 μg/ml of the ATP-synthase inhibitor oligomycin was added ($OCR_{O/L}$) followed by addition of 0.2 μM of the uncoupler carbonilcyanide p-triflouromethoxyphenylhydrazone (FCCP) (OCR_U). The rates of oxygen consumption were corrected for 2 μM antimycin A plus 2 μM rotenone-insensitive respiration and normalized to the initial cell number or mg protein.

2.5. Immunoblotting

Total protein extract from 10 [7] HepG2 cells was subjected to SDS-PAGE (12% acrylamide) and electroblotted by standard procedures. For *BMAL1* detection a rabbit polyclonal Ab (18,986-Abcam, dil. 1:1000) was used and a HRP-conjugated anti-rabbit IgG as secondary Ab (Thermo Scientific, dil. 1:20,000). Bands were visualized by chemiluminescence densitometric analysis (Versadoc Imaging System) and densitometric analysis of digitalized images carried out by Image J (http://imagej.nih.gov/ij/) and nomalized to anti-β-actin (1:10,000 mouse Ab from Sigma).

2.6. Real Time bioluminescence measuring

Lentiviral elements containing a *BMAL1*-promoter-driven luciferase (BLH) were generated as previously described [17]. HEK293T cells were seeded in 175 cm^2 culture flasks and co-transfected with 12.5 μg packaging plasmid psPAX, 7.5 μg envelope plasmid pMD2G and 17.5 μg *BMAL1*-promoter (BLH)-luciferase expression plasmid using the CalPhos mammalian transfection kit (Clontech) according to the manufacturer's instruction. To harvest the lentiviral particles, the supernatant was centrifuged at 4100 ×*g* for 15 min to remove cell debris and passed through a 45 μm filter (Sarstedt). The lentiviral particles were stored at −80 °C. For lentiviral transduction, 2×10 [5] HepG2 cells were seeded in 6-well plates in 1 ml medium and 1 ml of lentiviral particles was added; 8 μg/ml protamine sulfate (Sigma) was used to enhance transduction efficiency. The next day, the medium was replaced with selection medium (complete growth medium containing 100 μg/ml hygromycin B to obtain stable transduced cells and incubated at 37 °C with 5% CO_2 atmosphere. For bioluminescence measurement, 1.2×10 [6] transfected HepG2 cells were plated in 35 mm dishes (Thermo Scientific) one day prior to measurements. Cells were synchronized by serum shock as described above. Next, cells were washed once with

1× PBS and phenol-red-free DMEM supplemented with 250 μM D-Luciferin was added. *BMAL1*-promoter-(BLH)-reporter activity was measured, using a LumiCycle instrument (Actimetrics) for 5 days. Raw luminescence data were de-trended by subtracting luminescence counts by the 24 h running average using the LumiCycle software.

2.7. Cosinor analysis

The following equation was used to fit the experimental data from 0 to 24–30 h in synchronized cells: $f(t) = M + A\cos(t2\pi/P + \varphi) + st$; with M = mesor, A = amplitude, P = period, φ = acrophase, s = slope [18]. The best fit was attained using the software GraFit (V 4.0.13, Erithacus Software Limited).

2.8. Statistical Analysis

Experimental data are shown as mean ± standard error of the mean (SEM) with "n" indicating the number of independent experiments (i.e. non technical replicates). Data were compared by an unpaired Student-*t*-test or, when necessary, by 2-way ANOVA followed by a post-hoc Bonferroni test. Differences were considered statistically significant when the P value was less than 0.05. All analyses were performed using Graph Pad Prism (Graph Pad software, San Diego, CA, USA). Harmonic regression analysis of circadian oscillation of time-series data of gene expression was performed using CircWaveBatch V3.3 (http://www.euclock.org/results/item/circ-wave.html - Dr. RA Hut - University of Groningen) with a cut off P value of 0.05 and period length restricted to 24 or 48 h.

3. Results

3.1. Synchronized cultured HepG2 cells exhibit autonomous oscillatory mitochondrial respiratory activity

HepG2 cells were subjected to the well-established "serum shock" protocol shown to reset the clockwork machinery [15] thus allowing homogenous synchronization of the clock gene expression of cells in culture once the repressing condition is released. Fig. 1A illustrates the results of a systematic analysis whereby the cellular respiration was assessed in intact cells every three hours post-synchronization. The oxygen consumption rate, normalized to the cell number, was measured under the following conditions: a) under resting conditions relying on endogenous substrates (OCR_{RR}); b) following addition of the ATP-synthase inhibitor oligomycin, which is a measure of the respiratory activity controlled by ΔΨm-mediated proton leak across the membrane ($OCR_{O/L}$); c) following addition of the protonophore uncoupler FCCP (OCR_U) which elicits the maximal respiratory activity. By definition the difference $OCR_{RR} - OCR_{O/L}$ is a measure of the respiratory activity linked to the ATP-synthesis and the difference $OCR_U - OCR_{RR}$ is a measure of the respiratory reserve capacity (OCR_{RC}) [19]. Fig. 1A shows that, following synchronization, HepG2 cells displayed a rhythmic activity of respiration which peaked at the synchronization time (ST) of 12 h (first zenith). The OCR_{ATP} and OCR_{RC} measured at the zenith were significantly different from those measured at the two flanking nadirs (at ST of 6 and 18–21 h). The oscillatory activity in synchronized HepG2 cells can be better appreciated extending the observations over 48 h post-synchronization. As shown in the circular diagram of Fig. 1B three peaks alternating with a period of 13.6 ± 0.5 h (Cosinor fitting [18]) were clearly evident.

Analysis of the expression level of the master clock gene *ARNTL*/*BMAL1* resulted under identical conditions in an oscillatory profile both at the transcript and protein level (Fig. 1A,C). Notably, the zeniths of both the *BMAL1* mRNA and protein anticipated by three hours that of the respiratory activity. Analysis of the transcription of NR1D1 gene coding for REV-ERBα, negatively controlling the expression of *BMAL1*, resulted in an oscillatory profile which was out of phase deferred by 6 h with respect to *BMAL1* expression (Fig. 1A). Analysis of the time-series data of both gene expression (as well as of *BMAL1* protein and the OCRs of panels A and B) by 2-way analysis of variance resulted in significant change with time ($P < 0.05$). Moreover, harmonic regression analysis of the data performed using the CircWaveBatch software confirmed their statistically significant circadian oscillation.

The link between the rhythmic mitochondrial respiration and the clock genes was further analyzed in HepG2 cells where the expression of *BMAL1* was specifically inhibited by RNA interference. Fig. 1D shows that under conditions significantly reducing the expression of *BMAL1* the oscillation of the OCR_U was completely abrogated in synchronized HepG2 cells at the STs otherwise resulting in a significant oscillating activity in mock cells.

All together our experimental evidences suggest that *in vitro* synchronized cultured cells exhibit self-autonomous ultradian rhythmic oscillations of their mitochondrial respiratory activity linked to the expression of the core clock genes. This is a general phenomenon occurring irrespective of *i*) the cell type, *ii*) the respiratory carbon source, and *iii*) the protocol of synchronization (see ahead and [20]).

3.2. Expression of clock genes is affected by inhibitors of the mitochondrial OxPhos

Having attained indications that the biological clock controls mitochondrial respiration we reasoned to test whether OxPhos by its own exerted some regulatory function on the clock gene machinery. To this purpose HepG2 cells were synchronized in the presence of a subcytotoxic concentration of the respiratory chain inhibitor KCN. As expected, the respiratory activity was significantly inhibited (i.e. by about 50%) and, moreover, it lost any apparent time-dependent oscillatory profile (Fig. 2A); the cell viability was completely preserved over the 24 h post-synchronization. Most notably, the expression of *BMAL1* was depressed with apparent disappearance of the peak at 9 h post-synchronization (Fig. 2B). In a further set of experiments HepG2 cells were synchronized with low concentration of the protonophore uncoupler FCCP. Under this conditions the respiratory activity of synchronized cells was maximally stimulated but without any appreciable oscillatory profile over the 24 h post-synchronization (Fig. 2A). Importantly, FCCP treatment caused, alike KCN-treatment, the complete suppression of the rhythmic expression of *BMAL1* (Fig. 2B). Consistently, the *BMAL1* protein expression resulted inhibited in the post-synchronization period, following either KCN- and FCCP-treatment, and lose the marked oscillatory profile of the untreated synchronized cells (Fig. 2C).

To verify that the de-regulation of the rhythmic expression of *BMAL1* in OxPhos-inhibited cells persisted over a longer period, HepG2 cells were stably transfected with a *BMAL1*-promoter reported gene (i.e. (BLH)-luciferase) and the reporter activity measured by real time bioluminescence for 5 days post-synchronization. The results obtained confirmed a severe alteration of the expression profile of *BMAL1* (Fig. 2D).

Transcription of *NR1D1* (REV-ERBα) (Fig. 2E) as well as of RORα (data not shown) resulted severely suppressed in both KCN- and FCCP-treated cells indicating a general derangement of the clockwork machinery. The effect of the OxPhos inhibitors on gene expression appeared to be specific since transcription of the house-keeping genes TBS and 18S was unaffected (see inset of Fig. 2B).

3.3. Depletion of mtDNA in NHDF-neo impairs expression of the clock gene BMAL1

To support the indication that mitochondrial OxPhos influences the expression of the clockwork genes we generated fibroblasts specifically devoid of the mtDNA (i.e. Rho0-NHDF-neo) thereby unable to express catalytic subunits of the respiratory chain complexes I, III and IV as well as subunits of the ATP-synthase [16]. Fig. 3A shows that while synchronized parental NHDF-neo displayed a

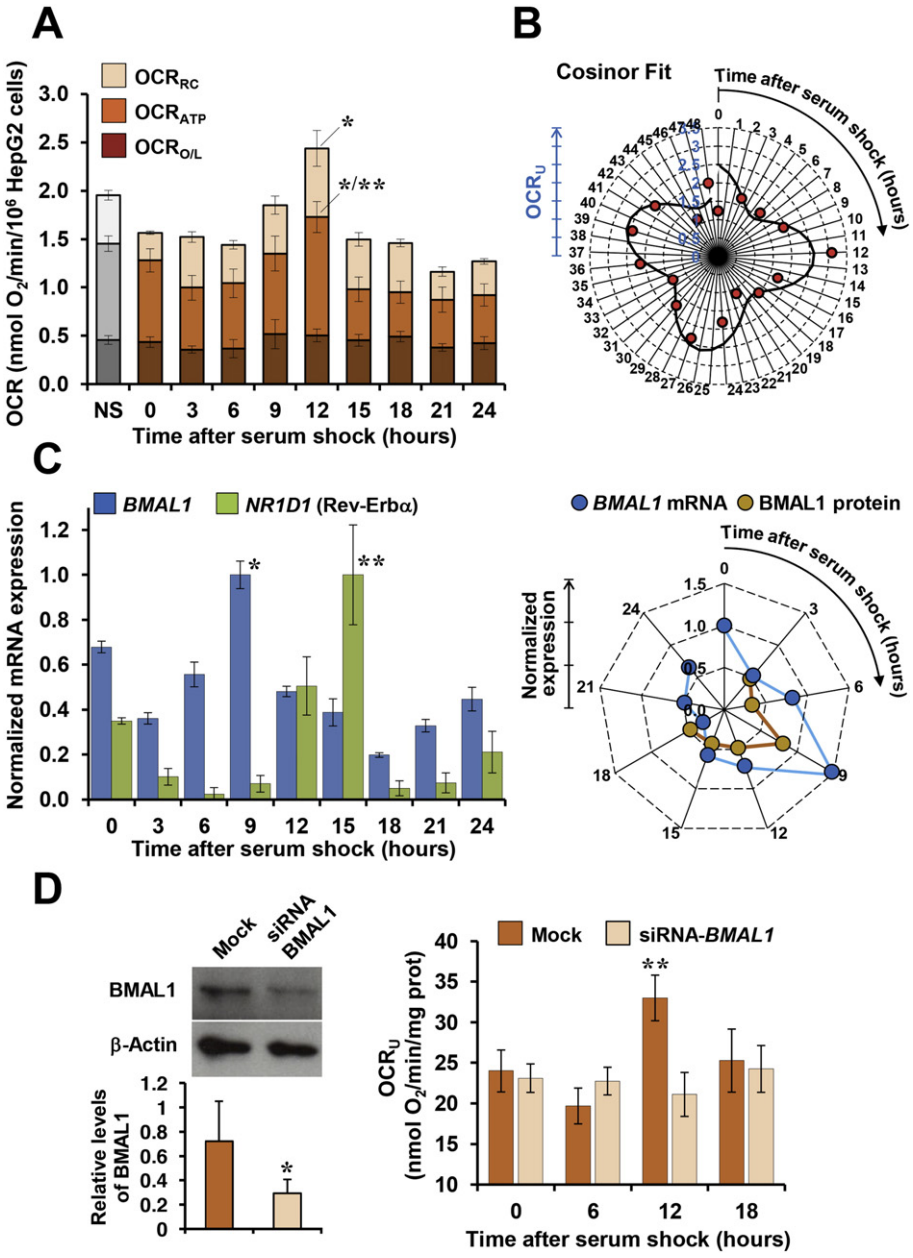

Fig. 1. Analysis of mitochondrial respiration and *BMAL1* expression in serum shocked synchronized HepG2 cells. **A** *Measurement of the mitochondrial respiratory activity in intact cells*. Histogram on the left: stacked bars indicate the oxygen consumption rate OCR with the subscripts "O/L", "ATP", "RS" referring to respiration in the presence of oligomycin controlled by proton leak, respiration dependent on the ATP synthase activity, reserve respiratory capacity respectively; NS, non synchronized cells; the values are means ± S.E.M. of n = 12 independent experiments; *, $P < 0.05$ for OCR_{RC} at ST = 12 *vs* ST = 0, 3, 6, 15, 18, 21, 24 and for OCR_{ATP} at ST = 12 *vs* ST = 0, 6, 9; **, $P < 0.01$ for OCR_{ATP} at ST = 12 *vs* ST = 3, 15, 18, 21, 24. B Circular diagram of the mitochondrial respiratory activity followed over 48 h post synchronization: red circles, OCR_U measured in the presence of the uncoupler FCCP normalized at ST = 0; means ± S.E.M. of n = 15 independent experiments (not technical replicate); continuous line, Cosinor best fit of the OCR_U with mesor = 2.00, amplitude = 0.61, period = 13.63, acrophase = 12.14, slope = 0.005. C *Expression of BMAL1 and NR1D1*. Histogram on the left: transcript level attained by q-RT-PCR of *BMAL1* and *ND1R1* (Rev-Erbα); values normalized to the zeniths are means ± S.E.M. of n = 3–4 independent experiments (three technical replicate each), *, $P < 0.05$ for both mRNAs *vs* all the other STs. Circular diagram on the right: comparison of the expression of *BMAL1* mRNA and protein level attained by q-RT-PCR and densitometric analysis of immunoblots respectively; values normalized to ST = 0 are means of n = 3 independent experiments (not technical replicates); *, $P < 0.05$ for both mRNA and protein at ST = 12 *vs* all the other STs. D *Effect of BMAL1 silencing on the OCR*. Left side: representative immunoblotting of *BMAL1* in HepG2 cells transfected with *siRNA-BMAL1* and densitometric analysis normalized to β-actin; means ± S.E.M. of n = 3; *, $P < 0.05$. Histogram on the right: uncoupled OCR_U in synchronized cells; means ± S.E.M. for n = 3 independent preparations; *, $P < 0.05$ of mock at ST = 12 *vs* both mock and siRNA-treated cells at all the other STs.

robust oscillatory respiratory activity, Rho0-NHDF-neo exhibited a faint OCR as expected from the almost complete depletion of the mtDNA. Most notably, the expression of *BMAL1*, although maintaining an oscillatory profile was substantially reduced in amplitude in Rho0-NHDF-neo as compared with parental cells (Fig. 3B) (statistical significance attained by both 2-way ANOVA and CircWaveBatch V3.3). No significant change in the expression of house-keeping genes was observed thus ruling out a generalized impairment of transcription. Collectively the results presented on one hand support the notion that the autonomous clock gene-dependent rhythmic activity of the mitochondrial OxPhos is a general phenomena occurring irrespective of the cell-type (i.e. cell lines vs primary cells), and on the other hand indicate that the timekeeping machinery is on its own controlled by the OxPhos system.

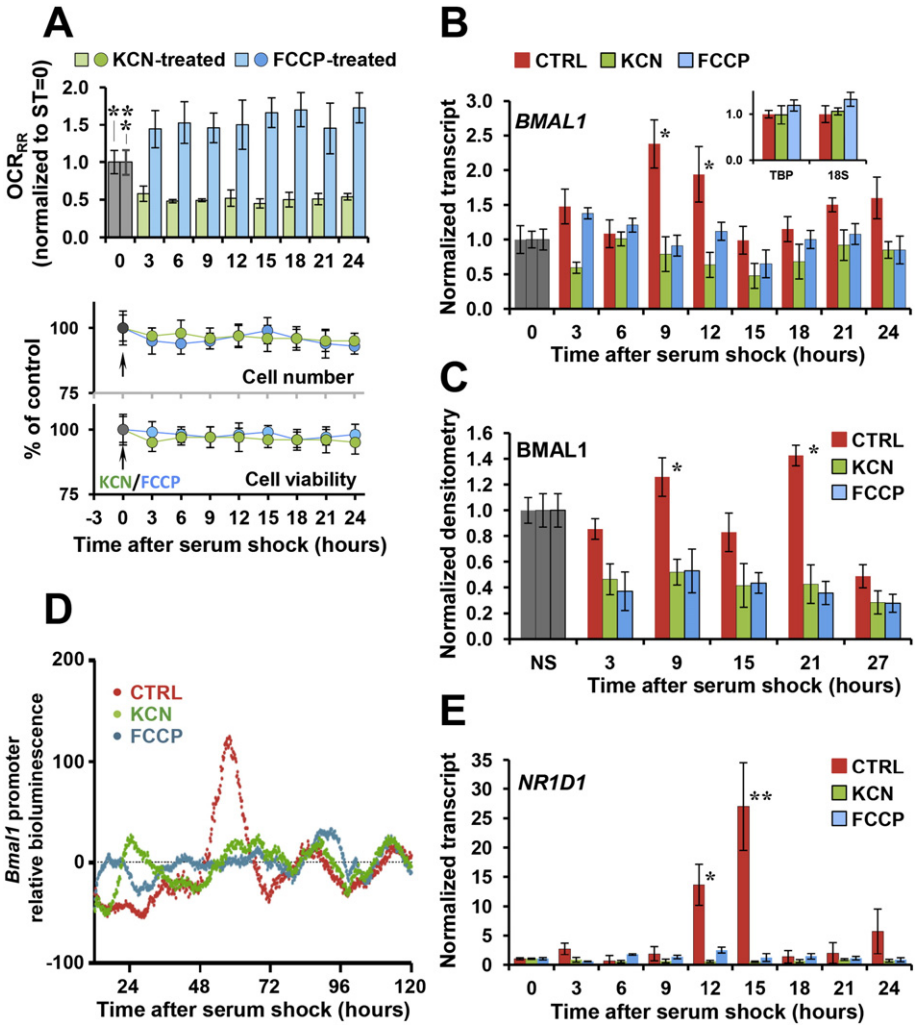

Fig. 2. Effect of mitochondrial OxPhos inhibition on the expression of *BMAL1*. Cells were treated either with 200 μM KCN or 0.2 μM FCCP at the onset of the serum-shock synchronization. A *Measurement of the OCR*. Histogram at the top: resting respiratory activity (OCR_{RR}) normalized to untreated cells (i.e. at ST = 0); means ± S.E.M. of n = 3; * $P < 0.05$, for the FCCP-treated cells at ST = 0 *vs* all the other STs; ** $P < 0.01$ for the KCN-treated cells at ST = 0 *vs* all the other STs. Graphs at the bottom: effect of KCN and FCCP on cell viability assessed by MTT assay and cell number assessed by visual counting; grey circles, untreated cell samples; means ± S.E.M. of n = 3. B *Expression of BMAL1*. Histogram showing *BMAL1* transcript level attained by q-RT-PCR; the values shown were normalized to ST = 0 and are means ± S.E.M. of n = 5–6 independent experiments (three technical replicate each); *, $P < 0.05$ for untreated at STs = 9–12 *vs* untreated and KCN-/FCCP-treated cells at all the other STs. The inset shows the normalized transcript levels of the TATA binding protein gene (TBP) and of the 18S ribosomal RNA (18S); means ± S.E.M. of n = 3 independent experiments (three technical replicate each). C *Expression of BMAL1 protein*. Densitometric analysis normalized to β-actin of immunoblots for *BMAL1* is shown; values were normalized to the protein level of non synchronized cells (NS) and are means of n = 3 independent experiments (not technical replicates); *, $P < 0.05$ at STs = 9–21 for untreated *vs* untreated and KCN−/FCCP-treated cells at all the other STs. D *Bioluminescence measurement of BMAL1 promoter-luciferase*. HepG2 cells were lentivirally transduced with a *BMAL1*-luciferase construct, synchronized and bioluminescence measured as described under Materials and Methods. Given are de-trended time series for one representative run/condition (a total of 3 runs/condition were carried out yielding similar results). Measurements for *BMAL1*-promoter activity were carried out for HepG2 cells (control, red) and following treatment with 0.2 mM KCN (green) or 0.2 μM FCCP (blue). E *Expression of NR1D1*. Histogram showing *NR1D1* transcript level attained by q-RT-PCR; the values shown were normalized to ST = 0 and are means ± S.E.M. of n = 3 independent experiments (three technical replicate each); *, $P < 0.05$ and **, $P < 0.01$ for untreated at STs = 12–15 *vs* untreated and KCN−/FCCP-treated cells at all the other STs.

4. Discussion

The present study implements the emerging notion that among the many functions circadianly controlled by clock genes the cellular metabolism occupies a central piece [10,11]. Given the pivotal role played by mitochondria as the cellular powerhouse it is not surprising that latest studies are focusing on the regulation of the oxidative metabolism by the clockwork machinery [12–14]. The novel contribution here provided is that, even in the absence of external cues or neuro-endocrine signals, likely every cell is equipped with autonomous ultradian oscillators rhythmically controlling the efficiency of the main ATP-generating system. Thus the central timekeeper accomplishes the function of synchronizing intrinsic bioenergetic oscillators opportunely matching/integrating their phases with periodic environmental changes.

The molecular basis linking the rhythmic expression of the clock-genes to the cellular metabolism is rapidly emerging. An interesting player in this scenario is provided by the NAMPT-NAD-SIRTs axis proved to undergo circadian oscillations under the control of the core clockwork genes [6,7,8,12,21]. In a parallel study carried out by our group we confirmed in synchronized in vitro models an oscillatory expression of *NAMPT* leading to fluctuating content of NAD which occurred synchronous with the rhythmic mitochondrial respiratory activity [20]. In addition to the recognized role played in the energy metabolism, NAD is also an essential cofactor in SIRT-mediated deacetylation processes [22]. Importantly, we found that the respiratory chain complex I underwent in synchronized cells an acetylation/deacetylation cycle, which led to its inhibition/activation respectively in phase with the nadirs and zeniths of the cellular respiration, and that activation of complex I was sensitive to SIRT inhibition [20]. All

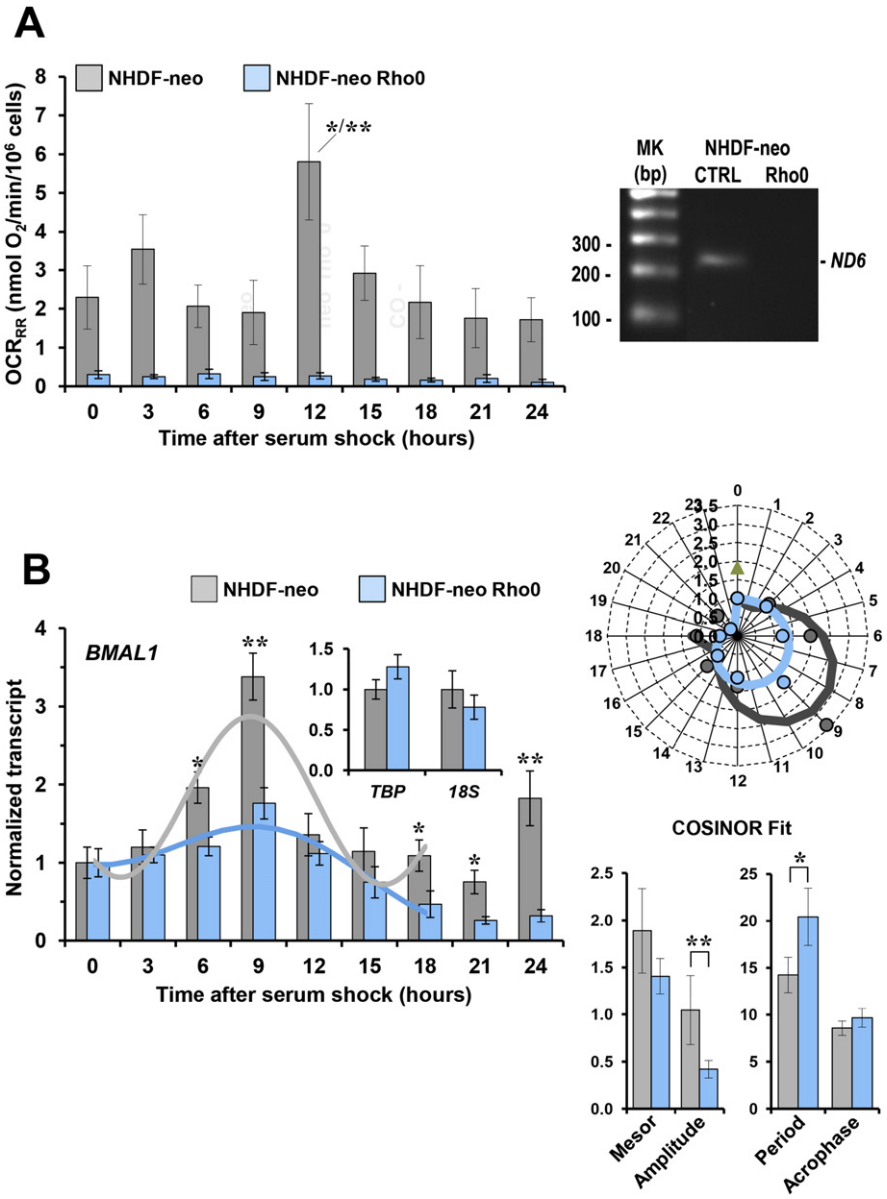

Fig. 3. Effect of mtDNA depletion in NHDF-neo on the expression of *BMAL1*. A *Measurement of the mitochondrial respiratory activity in intact cells*. Histogram on the left: resting respiratory activity (OCR_{RR}) in parental and Rho0-NHDF-neo; means ± S.E.M. of n = 3 independent experiments; *, P < 0.05 for NHDF-neo at ST = 12 *vs* ST = 0, 3, 15; **, P < 0.01 for NHDF-neo at ST = 12 *vs* ST = 6, 9, 18, 21, 24. Right side: agarose gel of the PCR-amplicon (35 cycles) for the mtDNA gene ND6; MK, molecular markers. B *Expression of BMAL1*. Histogram and circular diagram showing *BMAL1* transcript level attained by q-RT-PCR; values normalized to ST = 0 and means ± S.E.M. of n = 3 independent experiments (three technical replicate each); *, P < 0.05 and **, P < 0.01 for NHDF-neo *vs* Rho0-NHDF-neo at the indicated STs. The continuous lines in the circular diagram are the Cosinor best fits of the experimental points and the fitting parameter are comparatively shown in the bottom histogram; *, P < 0.05 and **, P < 0.01.

together these findings support a circadian control of the mitochondrial oxidative metabolism mediated by enhanced availability of the redox substrate NAD and by reversible post-translational modification of a respiratory chain complex (Fig. 4). It must be pointed out that additional circadian SIRT(s)-mediated activation of catabolic pathway(s), upstream of the respiratory chain, can contribute to modulate the mitochondrial oxidative performance as clearly shown for the fatty acid β-oxidation [12].

A further unexpected finding which emerged from the present study is that the circadian clock-controlled OxPhos regulates by its own the rhythmic expression of the core clock genes. This was demonstrated by the deregulating impact on the rhythmic *BMAL1* expression elicited by either KCN- and FCCP-treatment of synchronized cells. To note the mechanism of action of the two compounds is completely different in that one inhibits respiration activity blocking the terminal cytochrome c oxidase whereas the other accelerates the oxygen consumption rate collapsing the $\Delta\Psi_m$ which slows down the electron transfer throughout the respiratory chain [23]. The feature shared by the two experimental conditions tested (i.e. blocking *vs* uncoupling) is the inhibition of ATP synthesis by the OxPhos. Therefore, we suggest that the primary cause of the derangement of the core-clock machinery is conceivably represented by the bioenergetic fall *per se*. The less dramatic impact on the expression of *BMAL1* observed with Rho0-generated cells, as compared with the pharmacologic inhibitors, might be explained considering that while in the latter case an acute stress is imposed, in the long-lasting protocol to achieve depletion of the mtDNA cells may gradually adapt up-regulating glycolysis-mediated ATP production. To notice, ATP is a powerful activator of NAMPT [24] and is the co-substrate of the NAM-nucleotide adenylyltransferase NMNAT, a further enzyme involved in NAD biosynthesis, converting NMN in NAD.

The impact of our finding might provide suggestions in elucidating the cause–effect relationship of the observed disruption of the circadian

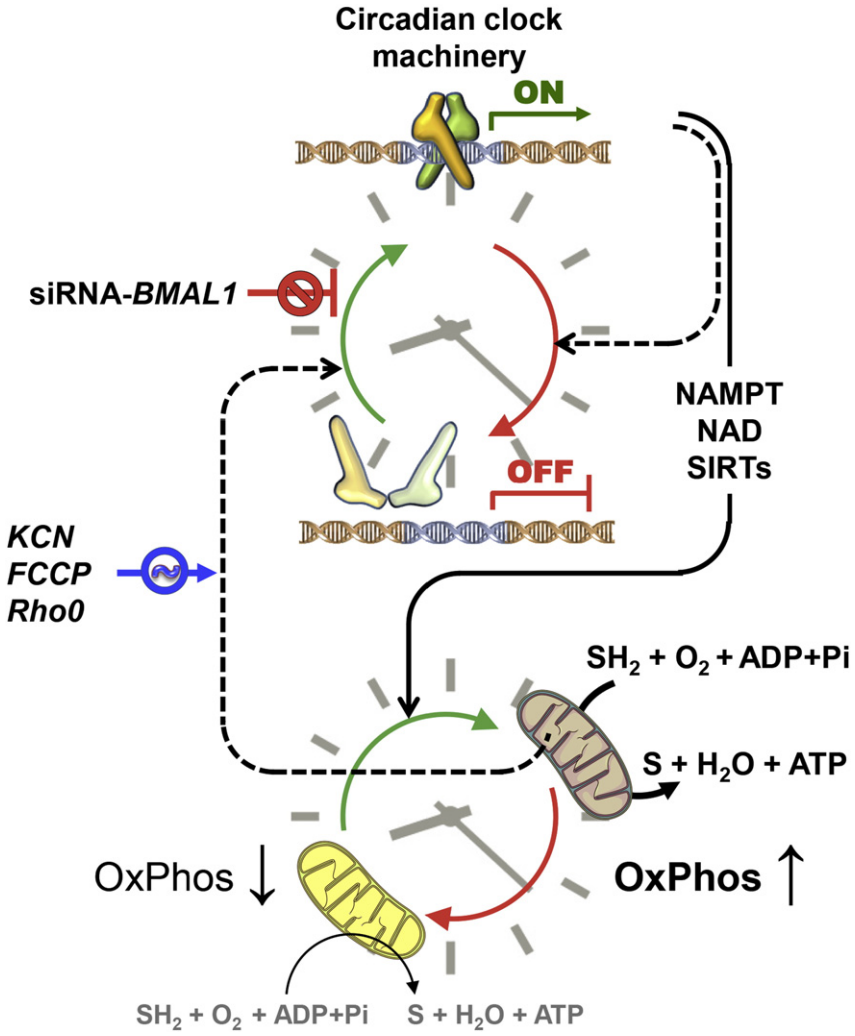

Fig. 4. Scheme showing the interlocked feedback loop controlling the interplay between cellular bioenergetics and circadian rhythmicty as inferred from the present study. Transcription factors involved in circadian rhythms timekeeping are shown alternating between active and inactive states. The NAMPT-NAD-SIRTs axis is rhythmically controlled by clock gene and shown to control the transition of mitochondria from a low to a high OxPhos performing state. In turn efficient mitochondrial activity positively controls the reactivation of the circadian clock machinery. The experimental conditions presented in this study to interfere with the reciprocal control are also shown. See Discussion for further details.

timekeeping in neurodegenerative diseases hallmarked by mitochondrial dysfunctions such as Alzheimer, Parkinson and Huntington diseases [25]. Scarce attention has been paid on alterations of circadian rhythms in patients affected by mitochondrial disorders and thus information in literature is lacking and this issue is object of hypothesis [26]. Nevertheless, in vivo experimentation clearly shows that mice treated with low dose of the respiratory chain toxin 3-nitropropionic acid exhibited severe circadian deficit in behavior [27]. Moreover, the recent finding of a crosstalk between circadian rhythmicity, mitochondrial dynamics/activity and macrophage bactericidal activity shed light on the timekeeping of the cell immune functions [28].

Although further studies are warranted to identify the molecular basis of the "retrograde" control of mitochondrial OxPhos in maintaining the time-keeping of intrinsic molecular clocks, our findings add a further level of complexity to the transcriptional-enzymatic feedback loop reciprocally interlocking cellular bioenergetics and circadian rhythmicty.

Author contributions

N.C. and G.Ma. generated the ideas and hypotheses, designed all experiments and analyzed data. R.S. and O.C. performed and designed most experiments under supervision of N.C. A.R. and L.F. designed, generated and analyzed the bioluminescence data. G.Me., B.A., G.Q., S.F., M.M., R.R. and C.P. participated in experimentation and discussions. N.C. and G.Ma wrote the manuscript.

Conflict of interest

The authors declare that they have no conflict of interest.

Transparency document

The Transparency document associated with this article can be found, in online version.

Acknowledgments

Financial support: the study was supported to N.C. by local grant of the University of Foggia (2014-15) through the Department of Clinical and Experimental Medicine; to G.Ma. by the "5 × 1000" voluntary contribution and a grant from the Italian Ministry of Health through Division of Internal Medicine and Chronobiology Unit (RC1203ME46, RC1302ME31, RC1403ME50, RC1504ME53), IRCCS "Casa Sollievo della Sofferenza", San Giovanni Rotondo (FG), Italy; to A.R. and L.F. by the German Federal Ministry of Education and

Research (BMBF)—eBio-CIRSPLICE—FKZ031A316, L.F. was additionally funded by the Berlin School of Integrative Oncology (BSIO) (2015) of the Charité Universitätsmedizin Berlin. The earlier contribution of Dr. Valerio Pazienza and Dr. Giorgia Benegiamo (Gastroenterology Unit, IRCCS "Casa Sollievo della Sofferenza", San Giovanni Rotondo (FG), Italy) to the development of this study is gratefully acknowledged.

References

[1] C. Dibner, U. Schibler, U. Albrecht, The mammalian circadian timing system: organization and coordination of central and peripheral clocks, Annu. Rev. Physiol. 72 (2010) 517–549.
[2] J.S. Takahashi, H.K. Hong, C.H. Ko, E.L. McDearmon, The genetics of mammalian circadian order and disorder: implications for physiology and disease, Nat. Rev. Genet. 9 (2008) 764–775.
[3] N. Preitner, et al., The orphan nuclear receptor REV-ERBalpha controls circadian transcription within the positive limb of the mammalian circadian oscillator, Cell 110 (2002) 251–260.
[4] U. Albrecht, Timing to perfection: the biology of central and peripheral circadian clocks, Neuron 74 (2012) 246–260.
[5] R. Zhang, N.F. Lahens, H.I. Balance, M.E. Hughes, J.B. Hogenesch, A circadian gene expression atlas in mammals: implications for biology and medicine, Proc. Natl. Acad. Sci. U. S. A. 111 (2014) 16219–16224.
[6] G. Asher, et al., SIRT1 regulates circadian clock gene expression through PER2 deacetylation, Cell 134 (2008) 317–328.
[7] Y. Nakahata, S. Sahar, G. Astarita, M. Kaluzova, P. Sassone-Corsi, Circadian control of the NAD+ salvage pathway by CLOCK-SIRT1, Science 324 (2009) 654–657.
[8] K.M. Ramsey, et al., Circadian clock feedback cycle through NAMPT-mediated NAD+ biosynthesis, Science 324 (2009) 651–654.
[9] B.M. Spiegelman, Transcriptional control of mitochondrial energy metabolism through the PGC1 coactivators, Novartis Found. Symp. 287 (2007) 60–63.
[10] J. Bass, J.S. Takahashi, Circadian integration of metabolism and energetics, Science 330 (2010) 1349–1354.
[11] J. Bass, Circadian topology of metabolism, Nature 491 (2012) 348–356.
[12] C.B. Peek, et al., Circadian clock NAD+ cycle drives mitochondrial oxidative metabolism in mice, Science 342 (2013) 1243417.
[13] D. Jacobi, et al., Hepatic Bmal1 regulates rhythmic mitochondrial dynamics and promotes metabolic fitness, Cell Metab. 22 (2015) 709–720.
[14] A. Neufeld-Cohen, et al., Circadian control of oscillations in mitochondrial rate-limiting enzymes and nutrient utilization by PERIOD proteins, Proc. Natl. Acad. Sci. U. S. A. (2016) (pii: 201519650 [Epub ahead of print]).
[15] A. Balsalobre, F. Damiola, U. Schibler, A serum shock induces circadian gene expression in mammalian tissue culture cells, Cell 93 (1998) 929–937.
[16] M.P. King, G. Attardi, Isolation of human cell lines lacking mitochondrial DNA, Methods Enzymol. 264 (1996) 304–313.
[17] S.A. Brown, et al., The period length of fibroblast circadian gene expression varies widely among human individuals, PLoS Biol. 3 (2005), e338.
[18] G. Cornelissen, Cosinor-based rhythmometry, Theor. Biol. Med. Model. 11 (2014) 16.
[19] B.K. Chacko, et al., The bioenergetic health index: a new concept in mitochondrial translational research, Clin. Sci. (Lond.) 127 (2014) 367–373.
[20] O. Cela, et al., Clock genes-dependent acetylation of complex I sets rhythmic activity of mitochondrial OxPhos, Biochim. Biophys. Acta 1863 (2016) 596–606.
[21] S. Masri, P. Sassone-Corsi, Sirtuins and the circadian clock: bridging chromatin and metabolism, Sci. Signal. 7 (2014) re6.
[22] H.C. Chang, L. Guarente, SIRT1 and other sirtuins in metabolism, Trends Endocrinol. Metab. 25 (2014) 138–145.
[23] D.G. Nicholls, S.J. Ferguson, Bioenergetics4, Academic Press, New York, 2014.
[24] E.S. Burgos, V.L. Schramm, Weak coupling of ATP hydrolysis to the chemical equilibrium of human nicotinamide phosphoribosyltransferase, Biochemistry 47 (2008) 11086–11096.
[25] A. Videnovic, A.S. Lazar, R.A. Barker, S. Overeem, 'The clocks that time us'—circadian rhythms in neurodegenerative disorders, Nat. Rev. Neurol. 10 (2014) 683–693.
[26] M.H. Hastings, M. Goedert, Circadian clocks and neurodegenerative diseases: time to aggregate? Curr. Opin. Neurobiol. 23 (2013) 880–887.
[27] T. Kudo, D.H. Loh, Y. Tahara, D. Truong, E. Hernández-Echeagaray, C.S. Colwell, Circadian dysfunction in response to in vivo treatment with the mitochondrial toxin 3-nitropropionic acid, ASN Neuro 6 (2014), e00133.
[28] J. Oliva-Ramírez, M.M. Moreno-Altamirano, B. Pineda-Olvera, P. Cauich-Sánchez, F.J. Sánchez-García, Crosstalk between circadian rhythmicity, mitochondrial dynamics and macrophage bactericidal activity, Immunology 143 (2014) 490–497.